

International Conference on Space Optics—ICSO 2008

Toulouse, France

14–17 October 2008

Edited by Josiane Costeraste, Errico Armandillo, and Nikos Karafolas



Enhanced broadband (11-15 μm) QWIP FPAs for space applications

Alexandru Nedelcu

Nadia Brière de l'Isle

Jean-Patrick Truffer

Eric Belhaire

et al.



International Conference on Space Optics — ICSO 2008, edited by Josiane Costeraste, Errico Armandillo, Nikos Karafolas, Proc. of SPIE Vol. 10566, 105662T · © 2008 ESA and CNES
CCC code: 0277-786X/17/\$18 · doi: 10.1117/12.2308223

Enhanced broadband (11–15 μm) QWIP FPAs for space applications

Alexandru Nedelcu⁽¹⁾, Nadia Brière de l'Isle⁽¹⁾, Jean-Patrick Truffer⁽¹⁾, Eric Belhaire⁽¹⁾, Eric Costard⁽¹⁾, Philippe Bois⁽¹⁾, Patrick Merken⁽²⁾, Olivier Saint-Pé⁽³⁾

(1) Alcatel-Thales III-V Lab, Route Départementale 128, 91767, Palaiseau Cedex, France

Email: alexandru.nedelcu@3-5lab.fr

(2) IMEC, Kapeldreef 75, B-3001 Leuven, Belgium

(3) Astrium SAS, 31 rue des Cosmonautes, Z.I. du Palays, 31402 Toulouse Cedex 4, France

ABSTRACT

A thirty months ESA project started in March 2008, whose purpose is to expand and assess the performance of broadband (11-15 μm) quantum detectors for spectro-imaging applications: Fourier Transform Spectrometers and Dispersive Spectrometers. We present here the technical requirements, the development approach chosen as well as preliminary signal to noise ratio (SNR) calculations. Our approach is fully compatible with the final array format (1024x256, pitch 50-60 μm). We expect the requested uniformity, operability and SNR levels to be achieved at the goal temperatures (60K for FTS applications and 50K for DS applications). The performance level will be demonstrated on 256x256, 50 μm pitch arrays. Also, operability and uniformity issues will be addressed on large mechanical 1024x256 hybrid arrays.

1. INTRODUCTION

For six years, the THALES Group has been manufacturing sensitive infrared arrays using Quantum Well Infrared Photodetectors (QWIP) technology at Alcatel-Thales III-V Lab (III-V Lab). After development and low-rate initial production (LRIP) phase in 2005, the first production stage of the QWIP based CATHERINE-XP thermal imager[1] by Thales Optronique SA (TOSA) started in 2006. The 384x288, 25 μm pitch, LWIR QWIP active layers are produced by the III-V Lab. The hybridisation step and the VEGA-LW-RM4 integrated dewar device cooler assembly (IDDCA) fabrication are done by Sofradir[2]. At 75K the IDDCA sensitivity is better than 30mK ($f/2.7$; $T_{\text{BKG}} = 293\text{K}$; instantaneous dynamic range $> +50^\circ\text{C}$; $T_{\text{INT}} < 7\text{msec}$). The same organization is now beginning for the production of the full TV 640x512, 20 μm pitch, SIRIUS-LW-K548 detector of Catherine MP. At 74K the IDDCA sensitivity is better than 30mK ($f/2.2$; $T_{\text{BKG}} = 293\text{K}$; instantaneous dynamic range $> +50^\circ\text{C}$; $T_{\text{INT}} < 7\text{msec}$).

The specific characteristics of QWIPs (GaAs-based III-V materials, easy wavelength adjustment through band-gap engineering, high thermal stability, high uniformity and yield, no low-frequency noise) pave the way to high performance imagers at mid-wave infrared (MWIR, 3-5 μm) and very long wave infrared (VLWIR, 10–20 μm) energies.

Large-format detectors in the 11-15 μm range with high radiometric and imaging performances are of increasing scientific and operational interest for, e.g., meteorology and atmospheric chemistry in missions such as Meteosat Third Generation (MTG) and other future Earth Observation (e.g. Post-EPS) or Planetary Science missions. Due to very stringent system requirements, the targeted performance levels can only be achieved with photon detectors with appropriate cooling ($\ll 77\text{K}$). Even so, the performance levels are challenging for the existing mature technologies.

The III-V Lab already fabricated and tested QWIP FPAs with cut-off wavelengths higher than 15 μm . Our first results in 2006 supported the feasibility of high operability ($>99.9\%$) and high uniformity ($\sigma/\text{mean}=4\%$) FPAs[3]. The operability and the electro-optical performance were improved in 2007, with several hybrid FPAs characterised and tested[4].

Recently the European Space Agency (ESA) has chosen a consortium led by the III-V Lab to develop enhanced broadband (11-15 μm) QWIP focal plane arrays for space applications. This article is devoted to the description of the project and of the retained development approach. In section 2 we describe the ESA project and explain why we retained the QWIP technology to answer the expressed needs. Section 3 is devoted to a detailed analysis of the technical requirements. Based on this analysis, a technological development approach is proposed in Section 4. Preliminary Signal to Noise Ratio (SNR) modelling and calculations are addressed in Section 5. The feasibility of QWIP arrays meeting the technical requirements is then discussed.

2. PROJECT DESCRIPTION AND CHOICE OF THE DETECTOR TECHNOLOGY

The overall purpose of the ESA project is to expand and assess the performance of broadband (11-15 μ m) quantum detectors for spectro-imaging: Dispersive Spectrometers (DS) and Fourier Transform Spectrometers (FTS). The primary objective is the development of an optimised detection layer, focusing on its technology and the necessary performance levels. The contract has been ascribed to a consortium composed of the III-V Lab (in charge of the active layer design and hybrid demonstrator manufacturing), IMEC (in charge of the read-out design and manufacturing) and Astrium SAS (in charge of electro-optical tests on hybrid demonstrators). The thirty months project started on March 13, 2008.

The primary objective of the proposed activity sets strong constraints on the detection layer technology:

- very low dark current or square resistance (R_0A);
- high absorption over an extended detection band;
- availability of large wafers (≥ 3 inches / 76mm);
- very uniform active layers over large surfaces ($>50 \times 15 \text{mm}^2$), leading to very low residual non-uniformities;
- negligible low-frequency noise, to guaranty performance stability (low drift between successive calibrations).

QWIPs are photoconductive infrared (IR) detectors behaving as non-linear resistors, not as diodes. The performance depends on the applied bias (typically 0.5 to 2.0 Volts). Absorption is based on a resonant electron transition between two confined levels of a quantum well: the responsivity is peaked at a given wavelength, with typical FWHM of 100 cm^{-1} (mostly independent on the peak wavelength). Broadband structures can easily be designed using alternating quantum wells with different quantum confinement characteristics. QWIPs sensing the 8-25 μ m range are made of AlGaAs/GaAs. They benefit from the mature processing technology of GaAs-based III-V compounds: large size wafers (up to 150mm diameter), excellent uniformity, high yield for large size components (e.g. FPAs), low cost. The use of molecular beam epitaxy (MBE) allows an excellent control of layer thickness (0.1 mono-layer), interface quality and residual impurity level (low 10^{14}cm^{-3} range). The peak wavelength can be continuously tuned from 8 μ m to more than 25 μ m, simply by decreasing the aluminium content in the barrier. The lower aluminium content leads to a higher material quality: VLWIR QWIPs are slightly easier to grow than LWIR QWIPs. Also, quantum well doping is even better mastered at lower aluminium contents (no deep impurity states in the barrier and larger wells).

The characteristics of QWIPs (dark current, absorption, gain) can be tuned in a fairly independent manner through the optimisation of parameters such as: number of wells, optical coupling scheme, doping level, potential profile in the barriers. The cut-off and cut-on wavelengths can be controlled either at the growth level or by varying the characteristics of the optical coupling scheme. The dark current in QWIPs has a physical origin and is process independent. It should not be considered as a leakage current (or shunt current) as for defective photovoltaic structures.

QWIPs are unipolar devices: only electrons take part to the transport. Passivation capping layers (as for MCT and Sb-based superlattices) are not needed. No other major processing challenges have to be addressed. Thanks to the well mastered growth and processing techniques, the dark current is highly uniform across the FPA. This feature is a strong advantage for VLWIR applications in terms of performances and in flight calibration strategy, as the system performances are often limited by spatial noise (differential dark current noise) introduced by large DSNU coupled to focal plane temperature instabilities. Static resistance (V/I) as well as dynamic resistance (dV/dI) are very large for QWIP structures ($> 100 \text{M}\Omega$). This should avoid the need for special injection stage designs, on the contrary of 2D array VLWIR MCT.

QWIPs exhibit a true white noise. No low frequency ($1/f$ noise) has been evidenced in regular structures. This leads to very stable temporal characteristics, simplified image correction procedures, better system performances and relaxation of the in-flight calibration strategy. Unlike photovoltaic structures (with photoconductive gain $g = 1$), QWIPs exhibit very low photoconductive gains (< 0.5). This impacts the peak responsivity as well as the noise level. Low gain detectors may lead to improved performance compared to photovoltaic detectors.

QWIPs are the III-V Lab industrial choice. For the proposed activity we retain the QWIP technology and develop the roadmap to reach the performance level suitable for ESA applications.

3. ANALYSIS OF THE TECHNICAL REQUIREMENTS

In this section we review the main Technical Requirements, as given in the Invitation to Tender.

- FPA final format and pitch (1024x256, 50-60 μ m pitch): achievable with the present QWIP technology even on 3" wafers (two full-format FPAs per wafer). The final format read-out requires stitching which is

offered for the pre-selected 0.35 μ m CMOS process. We therefore expect that the read-out size will not be a challenge. Critical points are identified rather at the hybridisation step. Solutions do exist to deal with the thermal mismatch between GaAs and Si.

- Fill factor (threshold: >90%; goal: >98%): the currently achieved value is higher than 92% for a 50-60 μ m pitch. Thanks to the mesa geometry QWIPs do not exhibit any cross-talk (electrical, optical). Values higher than 98% lead to a very challenging separation between pixels (500 nm) while bringing only very slight improvement.

- Flatness (threshold: < +/- 5 μ m; goal: < +/- 2.5 μ m): the goal value is today achieved after the hybridisation step.

- Spectral range (11-15 μ m): the required spectral range can be achieved with either a broadband QWIP structure (FTS applications) or with a two-stack multi-colour QWIP pixel structure plus optical coupling structure progressively varying along the structure (DS applications).

- Signal to noise ratio (threshold for FTS: 2150@60K; threshold for DS: 700@50K): will be discussed in Section 5.

- Quantum efficiency and dark current (goal: 50%, 86 fA/ μ m²): absorption (rather than external quantum efficiency) is relevant for QWIPs, due to a low photoconduction gain. Values higher than 50% on 50 μ m pixels can be achieved. Optimisation efforts are needed for both the active layer and optical coupling scheme. Optical coupling optimisation will allow maintaining / decreasing dark current, while increasing absorption. For a given quantum structure and doping level the achieved dark current depends on the applied bias and operating temperature. The goal value is challenging with respect to measured values in non optimised QWIPs (1 pA/ μ m² at 50K, cut-off at 15 μ m).

- Read-out noise (goal: 50 electrons): for a 50 μ m pitch the integration capacitor will be 5-10 pF (reset noise between 370 and 520 electrons). A noise of 50 electrons requires the implementation of specific functions (correlated double sampling). However, the analogue signal processing chain will likely be the dominant noise source. We estimate that the read-out noise will not limit the overall performance so much.

- Dynamic range (threshold: 80dB; goal: 85dB): defined as the ratio between maximum handling charge divided by readout noise. For a 2V dynamic voltage, a 200 μ V total readout noise (80dB) is not challenging. The goal value (85dB, 112 μ V read-out noise) will be hard to achieve, especially for high frame rate as needed for FTS applications.

- Charge handling: charge handling capacities of 50-100 Mega-electrons for a 50-60 μ m pitch are

currently achievable. These values are compatible with the required performance level.

- Read-out mode (snapshot): not critical. Snapshot + 'integrate while read' is feasible, but will have an impact on other parameters as linearity, charge handling and noise.

- Photo-Response Non-Uniformity (PRNU; threshold: <1%; goal: < 0.1%): the threshold value is reachable with the existing technology, at the operating temperature (60K for FTS, 50K for DS). 0.1% rms looks challenging.

- Dark Signal Non-Uniformity (DSNU; threshold: <10%; goal: <1%): values lower than 5% are the standard for the QWIP technology and should be achieved at the operating temperature (60K for FTS, 50K for DS). Values lower than 1% are within reach for QWIPs thanks to the excellent uniformity of the MBE technique. Moreover, this parameter for the QWIP technology exhibits a very high temporal stability.

- Defects (threshold: <0.1% @ 3 σ ; goal: <0.1% @ 2 σ): our 8-10 μ m 640x512 FPAs achieve less than 0.1% of pixels at more than 2 σ outside the specifications. The requested operability levels are already achieved. As growth and processing of 15 μ m QWIPs are less demanding, this item seems not critical up to 60K, whatever the application.

- Modulation Transfer Function (MTF; >55%): for LWIR QWIP products (pitch 25 μ m; fill factor > 90%) the MTF@Nyquist is higher than 60%. A MTF@Nyquist higher than 55% is not critical for VLWIR and 50 μ m pitch.

- Power dissipation (< 200mW): the specified value seems feasible; however a careful trade-off should be made when considering the higher frame rate required for FTS applications.

4. DEVELOPMENT APPROACH

In this section we present the focal plane array architectures as well as the development approach (active layer + read-out) retained for this work. It has been decided to develop, manufacture and test the following demonstrators:

- a 256x256, 50 μ m pitch, performance demonstrator for FTS applications, based on an optimised QWIP active layer;

- a 256x256, 50 μ m pitch, performance demonstrator for DS applications, based on an optimised QWIP active layer;

- a large format (1024x256, 50 μ m pitch), hybridised QWIP array on silicon substrate (no read-out, but possibility to test several hundreds of pixels to address operability and uniformity issues).

FTS applications require a uniform, truly broadband FPA. All the pixels forming the FPA must be identical. The solution retained is fully compatible with a 1024x256, 50 μ m pitch format. We will implement a broadband QWIP active layer. The currently available technology allows the coverage of the 11–15 μ m band with a single stack structure. Broadband absorption is achieved by alternating quantum wells with different transition energies (see Fig. 1). The "unit cell" used to build the active layer may contain two, three or more quantum wells. If needed, all the QWs in the structure may be different. The unit cell will impact on the precise spectral shape as well as the dark current characteristics. Several approaches are retained:

- unique AlGaAs alloy for the barriers and different alloy compositions for the wells (AlGaAs / InGaAs);
- several barrier and well compositions, leading to complex confining potential shapes.

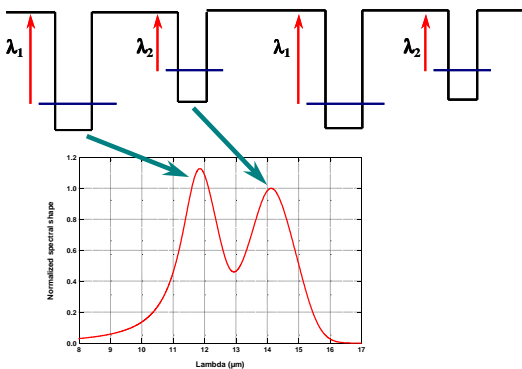


Fig. 1 FTS applications: example active layer

For DS applications the designed focal plane array will exhibit a varying spectral response along one direction (smoothly varying peak wavelength across rows, uniform spectral shape within a given row). The solution detailed below is fully compatible with a 1024x256, 50 μ m pitch format. We will implement a double stack quantum structure. The lower quantum well stack covers the 11–13 μ m spectral range while the upper stack covers the 13-15 μ m range. The double stack detector layer and corresponding processing steps have already been developed and evaluated at the III-V Lab, for MWIR/LWIR bi-spectral demonstrators with a pitch of 25 μ m. They will be adapted to the present project. For a 1024x256 dispersive array we will design a FPA architecture based on the division of the 2D array into two halves (512x256), on the same chip. One half will exploit the upper quantum well stack, the second half being processed to use the lower stack. Each half-FPA will be fitted with optimised diffraction gratings, whose periodicity will be varied across the array (from one row or a group of rows to another). The concept is illustrated in Fig. 2. For a given half-

FPA all the pixels will exhibit the same dark current and photoconductive gain.

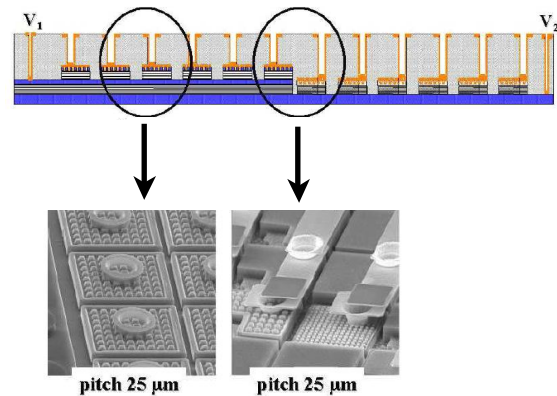


Fig. 2 FPA architecture for DS applications and already achieved results (exp. results from III-V Lab)

Whatever the final application, the two 256x256 performance demonstrators will be designed to test several read-out topologies. To do that we divide the arrays into 4 blocks of 64 columns. For the FTS demonstrators all the pixels will be nominally identical (same dark current, same spectral shape). A sketch of the array layout is shown in Fig. 3. For the DS demonstrators we will reproduce the architecture of a full format array (all the pixels will be nominally identical within a row, the optical coupling will be varied along the rows). A sketch of the array layout is shown in Fig. 4. For both architectures blind pixels are implemented outside the array. They will be used for skimming architectures. To ensure that these pixels are really blind we will hide them with a metallic layer deposited on the backside of the detection circuit.

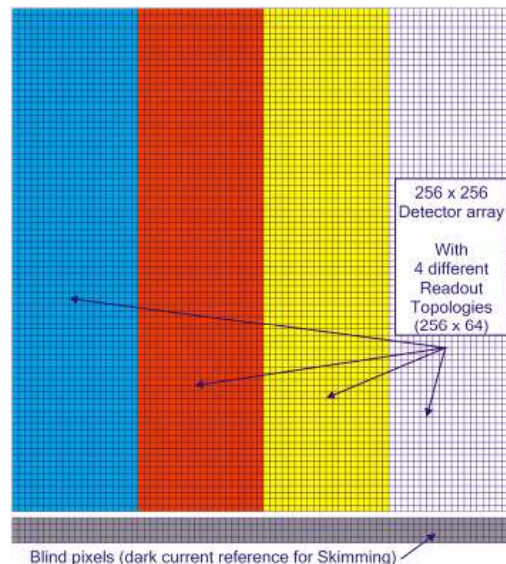


Fig. 3 Global layout for FTS demonstrators

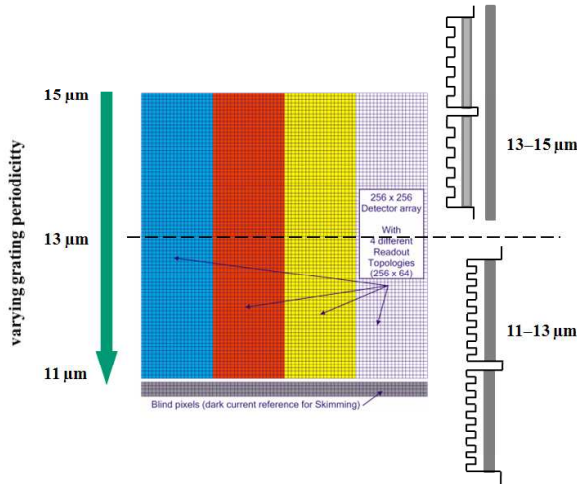


Fig. 4 Global layout for DS demonstrators

Several independent parameters are available to optimise the performance of the QWIP active layers. number of wells, well doping, precise unit cell potential profile, barrier width, optical coupling ... A key point is the design of the optical coupling scheme. Quantum wells weakly absorb radiation at normal incidence. However, if the radiation electric field is perpendicular to the QWs, the absorption is very strong, even for a low QW doping level. Appropriate numerical simulation tools are available at the III-V Lab, that allow the study of finite size, arbitrary shape, 3D objects (e.g. pixel + optical coupling). As we show in Section 4, the main performance limitation comes from the dark current level. Active layer design efforts will concentrate on this point. Also, maximising the well capacity on the read-out will contribute to increasing the performance.

The following roadmap has been set:

- step 1: active layer optimisation; read-out predevelopment; optimisation of specific technological steps (implementation of blind pixels; broadband anti-reflection coating; hybridisation with a pitch of 50μm; grating pattern transfer for DS architectures; mastering of the topology for the double stack DS architecture);
- step 2: QWIP array and FPA design; read-out design;
- step 3: QWIP active layer manufacturing; read-out manufacturing; hybrid FPA realisation;
- step 4: tests.

5. SIGNAL TO NOISE RATIO: PRELIMINARY ESTIMATIONS

To calculate the Signal To Noise Ratio (SNR) we first define the parameters needed to build a parametric performance model. Next we quickly show how the SNR must be calculated for QWIP detectors. We

present preliminary SNR calculations based on non optimised QWIP active layers and read-out. Finally, we estimate the optimisation effort needed to meet the technical requirements.

The design of a typical model sounder instrument will provide a quantitative definition of the following parameters: maximum integration time (t_{INT}^{MAX}); operating temperature (T_{FPA}); spectral range, defined between a minimum (λ_{MIN} , and a maximum (λ_{MAX}) wavelength; spectral density of the incoming flux for FTS ($dP/d\lambda(\lambda)$, W/m²/μm); incoming flux for DS (P , W/m²). Values for the background (BKG), signal (SGN) and maximum signal (SGNMAX) are needed. The values defined in the technical requirements are given in Table 1.

Table 1 System input parameters

FTS applications		DS applications	
Param.	Value	Param.	Value
$dP_{BKG}/d\lambda$	0.1 W/m ² /μm	P_{BKG}	0.013 W/m ²
$dP_{SGN}/d\lambda$	0.125 W/m ² /μm	P_{SGN}	0.0015 W/m ²
$dP_{SGN}^{MAX}/d\lambda$	0.175 W/m ² /μm	P_{SGN}^{MAX}	0.003 W/m ²
t_{INT}^{MAX}	2.2 msec	t_{INT}^{MAX}	42 msec
T_{FPA}	> 60K	T_{FPA}	> 50K

The QWIP detector is characterised by the following parameters: pixel area (S_D); applied bias (V); dark current density (J_{DARK}); photoconduction gain (g_N); peak responsivity (R_{PEAK}); normalised spectral shape ($R_{NORM}(\lambda)$). The read-out circuit is characterised by the following parameters: charge handling capacity (N_{ROIC}); read-out noise (B_{ROIC}); skimming current (I_{SKIM}). I_{SKIM} is the current that can be subtracted from the total current in order to increase the integration time

The signal to noise ratio (SNR) is given by:

$$SNR = (I_{BKG} + I_{SGN}) / \delta I_{TOT} \quad (1)$$

I_{BKG} is the optical current due to the background flux. I_{SGN} is the optical current due to the signal flux. δI_{TOT} stands for the total noise (detector + read-out). To calculate the noise one needs the expression of the detector noise spectral density (NSD, A/√Hz). For QWIPs, it can be written as:

$$NSD = \sqrt{4 \cdot e \cdot g_N \cdot I_{TOT}} \quad (2)$$

where I_{TOT} is the total current flowing through the active layer. We take into account that thermal noise as well as low-frequency noise are negligible in QWIPs.

The total current flowing through the detector takes into account the dark current and the optical current. The maximum total current is:

$$I_{TOT}^{MAX} = I_{DARK} + I_{BKG} + I_{SGN}^{MAX} \quad (3)$$

The total current under normal operating conditions is:

$$I_{TOT} = I_{DARK} + I_{BKG} + I_{SGN} \quad (4)$$

If a maximum value (t_{INT}^{MAX}) is imposed, then the integration time is:

$$t_{INT} = \text{MIN} \left(t_{INT}^{MAX}, (e \cdot N_{ROIC}) / (I_{TOT}^{MAX} - I_{SKIM}) \right) \quad (5)$$

By construction (skimming architecture, read-out architecture), one has $I_{TOT}^{MAX} > I_{SKIM}$ and the integration time is always defined and positive.

If skimming is performed the total current noise is:

$$\delta I_{TOT} = \sqrt{\frac{4 \cdot e \cdot g_N \cdot I_{TOT} + 2 \cdot e \cdot I_{TOT}}{2 \cdot t_{INT}} + \left(\frac{e \cdot B_{ROIC}}{t_{INT}} \right)^2} \quad (6)$$

We performed a preliminary estimation of the SNR, based on two non-optimised active layers (one for each architecture). The electro-optical characteristics of these initial active layers have been published elsewhere [5]. These layers do not represent the state of the art but are derived from existing layers studied at the III-V Lab. Moreover, we voluntarily degraded their performance, in order to set a lower limit to the achievable SNR. We retain the following parameters for the read-out circuit: pitch **50µm**; maximum charge handling capacity **50e6 electrons**; read-out noise: **500 electrons**.

The calculated performance is reported in Table 2. The optimum applied bias depends on the temperature and remains lower than 1.5 Volts. As expected, the initial active layers do not meet the technical requirements. Yet, they set a lower limit to the achievable performance. They also suggest that DS arrays are more challenging than FTS arrays.

Based on the obtained results, we elaborated an optimisation strategy for each of the active layers. In the following we present the calculated performance

achieved after moderate optimisation efforts, corresponding to a high confidence level. We also indicate what is the ultimate optimisation effort needed to meet the technical requirements. At this point we still do not take into account the performance improvement due to read-out circuit optimisation.

Table 2 SNR calculations: lower limit from non optimised structures

FTS		DS		
T _{FPA}	SNR	T _{FPA}	SNR 11-13µm	SNR 13-15µm
48K	2500	44K	> 430	> 210
50K	1900	46K	> 270	> 115
52K	1300	48K	> 150	> 70
54K	900	50K	> 80	> 45
56K	600	52K	> 50	> 30
58K	400			
60K	300			

After moderate (high confidence level) optimisation efforts on the active layer the following improvement of the electro-optical characteristics is expected:

- FTS active layer: $R_{PEAK} \times 1.6$; $g_N / 1.5$; $J_{DARK} / 2.5$;
- DS active layer, 11-13µm stack: $R_{PEAK} \times 2.5$; $g_N / 1.5$; $J_{DARK} / 2.0$;
- DS active layer, 13-15µm stack: $R_{PEAK} \times 2.4$; $g_N / 2$; $J_{DARK} / 4.0$.

The corresponding SNR calculation are given in **Table 3**. The technical requirements are met above 56K for FTS arrays and above 47K for DS arrays.

Table 3 SNR calculations: levels achieved after moderate optimisation efforts

FTS		DS		
T _{FPA}	SNR	T _{FPA}	SNR 11-13µm	SNR 13-15µm
48K	5800	44K	>1600	>1600
50K	4900	46K	>1000	>1100
52K	3600	48K	>650	>650
54K	2900	50K	>400	>300
56K	2200	52K	>200	>150
58K	1600			
60K	1100			

After ultimate optimisation efforts on the active layer the following improvement of the electro-optical characteristics is expected:

- FTS active layer: $R_{PEAK} \times 2$; $g_N / 1.5$; $J_{DARK} / 5$;
- DS active layer, 11-13µm stack: $R_{PEAK} \times 3$; $g_N / 1.5$; $J_{DARK} / 3$;
- DS active layer, 13-15µm stack: $R_{PEAK} \times 3$; $g_N / 2$; $J_{DARK} / 10$.

The corresponding SNR calculation are given in Table 4. The technical requirements are met above 60K for FTS arrays and above 50K for DS arrays.

Table 4 SNR calculations: with ultimate optimisation efforts

FTS		DS		
T _{FPA}	SNR	T _{FPA}	SNR 11-13µm	SNR 13-15µm
48K	7500	44K	>2300	>2700
50K	6500	46K	>1600	>2100
52K	5300	48K	>1050	>1350
54K	4500	50K	>700	>750
56K	3400	52K	>400	>500
58K	2600			
60K	2200			

If realistic read-out optimisation is taken into account (charge handling up to 100e6 electrons, read-out noise down to 200 electrons), the calculated performance is increased by 20-30%. This improvement corresponds to more than 1K increase in the operating temperature and correspondingly lower constraints on the active layer.

In the present state of knowledge we estimate that a SNR level of 700 can be achieved at 48-49K for the DS architecture. This estimation holds for a fully optimised QWIP active layer and read-out. The confidence level is close to 100%. Operation at 50K without SNR degradation is possible but will require careful optimisation of the active layer, especially of the 13-15µm stack.

For the FTS architecture we estimate that a SNR level of 2150 can be achieved at 58K. This estimation holds for a fully optimised QWIP active layer and read-out. The confidence level is close to 100%. Operation at 60K without SNR degradation is possible but will require careful optimisation of the active layer.

We also note that parameters such as DSNU, PRNU and defects are only slightly impacted by the choice of the active layer. Consequently, the achievable uniformity and operability should not depend much on the temperature.

6. CONCLUSION

The technical requirements and the development roadmap for achieving high performance broadband (11-15µm) quantum detectors for spectro-imaging applications have been addressed. No technological blocking points have been identified. The requested uniformity (DSNU, PRNU) and operability (defects) levels do not appear as challenging. Yet, from preliminary performance estimations, the required performance level (SNR) appears as challenging with respect to the operating temperature. We expect the

requested SNR level to be achieved above 58K for FTS applications and above 48K for DS applications. Operation at the goal FPA temperature (60K for FTS, 50K for DS) is possible after careful optimisation of both the active layer and read-out. These conclusions will be reconsidered after characterisation of dedicated samples.

The performance will be demonstrated on 256x256, 50µm pitch hybrid FPAs. Uniformity and operability issues will be addressed on a mechanical 1024x256 hybrid.

7. ACKNOWLEDGEMENTS

This work is supported by ESA under contract no 21248/08/NL/IA.

REFERENCES

- [1] S. Crawford et al., "THALES long-wave advanced IR QWIP cameras", Proc. SPIE 6206, 62060H (2006)
- [2] A. Manissadjian et al., "Single color and dual-band QWIP production results", Proc. SPIE 6206, 62060E (2006)
- [3] E. Costard et al., "QWIP from 4µm up to 18µm", Proc. SPIE 6361, 6361-17 (2006)
- [4] E. Costard et al., "Focal Plane Arrays from UV up to VLWIR ", Proc. SPIE 6744, 674411 (2007)
- [5] A. Nedelcu et al., "Enhanced broadband (11–15 µm) QWIP FPAs for space applications", Proc. SPIE 7106, 7106-57 (2008)